Powerful images.
Clear answers.

HOLOGIC®
The Science of Sure
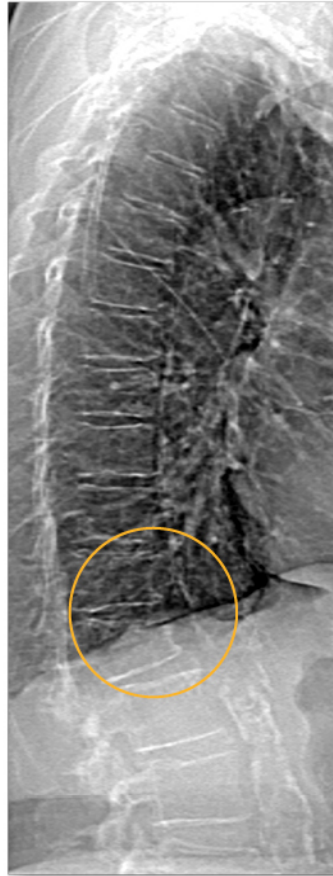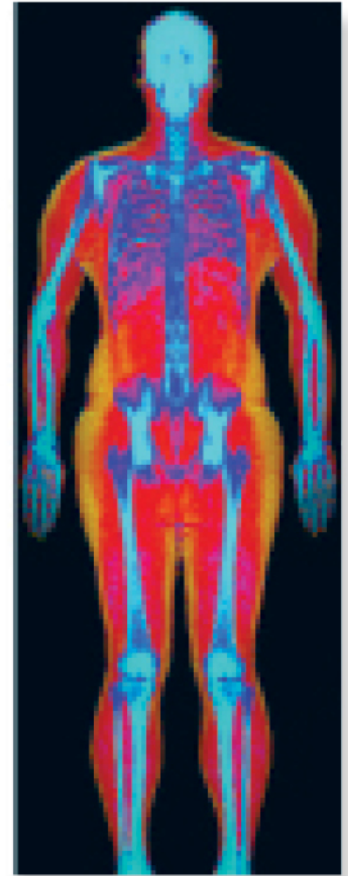
Manage Patient's concerns about Atypical Femur Fracture*

Vertebral Fracture Assessment – a critical part of a complete fracture risk assessment

Advanced Body Composition® Assessment – the power to see what's inside

Contact your Hologic rep today at BSHSalesSupportUS@hologic.com

PAID ADVERTISEMENT

www.hologic.com | dxaperformance.com | 1.800.442.9892

Identifying a Molecular Phenotype for Bone Marrow Stromal Cells With In Vivo Bone-Forming Capacity

Kenneth H Larsen,[1] Casper M Frederiksen,[1] Jorge S Burns,[1] Basem M Abdallah,[1] and Moustapha Kassem[1,2]

[1]Laboratory for Molecular Endocrinology (KMEB), Department of Endocrinology, University Hospital of Odense and Medical Biotechnology Center, University of Southern Denmark, Odense C, Denmark
[2]Stem Cell Unit, Department of Anatomy, College of Medicine, King Saud University, KSA

ABSTRACT

The ability of bone marrow stromal cells (BMSCs) to differentiate into osteoblasts is being exploited in cell-based therapy for repair of bone defects. However, the phenotype of ex vivo cultured BMSCs predicting their bone-forming capacity is not known. Thus we employed DNA microarrays comparing two human bone marrow stromal cell (hBMSC) populations: One is capable of in vivo heterotopic bone formation (hBMSC-TERT^{+Bone}), and the other is not (hBMSC-TERT^{-Bone}). Compared with hBMSC-TERT^{-Bone}, the hBMSC-TERT^{+Bone} cells had an increased overrepresentation of extracellular matrix genes (17% versus 5%) and a larger percentage of genes with predicted SP3 transcription factor–binding sites in their promoter region (21% versus 8%). On the other hand, hBMSC-TERT^{-Bone} cells expressed a larger number of immune-response-related genes (26% versus 8%). In order to test for the predictive value of these markers, we studied the correlation between their expression levels in six different hBMSC-derived clones and the ability to form bone in vivo. We found a significant correlation for decorin, lysyl oxidase-like 4, natriuretic peptide receptor C, and tetranectin. No significant positive correlation was found for canonical osteoblastic markers Runx2, alkaline phosphatase, collagen type I, osteopontin, and bone sialoprotein. Prospective isolation of four additional hBMSC clones based on their expression levels of the molecular markers correlated with their in vivo bone-formation ability. In conclusion, our data suggest an in vitro molecular signature predictive for hBMSCs' in vivo bone-formation ability. Identifying more of these predictive markers would be very useful in the quality control of osteoblastic cells before use in therapy. © 2010 American Society for Bone and Mineral Research.

KEY WORDS: BONE MARROW STROMAL CELLS (BMSCs); OSTEOBLAST; BONE FORMATION; BIOMARKERS; DNA MICROARRAYS

Introduction

During bone turnover and repair in the postnatal organism, osteoblasts are derived from bone marrow stromal cells (BMSCs; also known as *mesenchymal stem cells* and *skeletal stem cells*) that reside in the nonhematopoietic compartment of bone marrow stroma.[1–4] BMSCs are capable of multilineage differentiation into various mesoderm-type cells, including osteoblastic cells.[5,6] This ability has been used in cell-based therapy for a variety of bone diseases, for example, repair of bone defects and nonhealed fractures.[6–8] However, human BMSCs (hBMSCs) are heterogeneous, and not all the cells maintained under standard culture conditions are capable of bone formation.[4] Thus the efficient use of hBMSCs in therapy requires identification of an ex vivo cellular phenotype predictive of the ability of hBMSCs to form bone when implanted in vivo, that is, identifying

phenotypic and biomarkers associated with commitment of hBMSCs to the osteoblastic cell lineage.

The cellular and molecular phenotype of osteoblastic cells usually is defined in terms related to their functions. Osteoblasts and their progenitors exert a multitude of biologic functions.[9] They are responsible for bone formation during bone remodeling, they control osteoclastic cell functions through secretion of a large number of cytokines, and they support hematopoiesis by providing a supportive niche.[10] Nevertheless, the ability to form bone in vivo is considered the bona fida characteristic of osteoblastic cells.[9] Bone formation is a complex process that involves several cellular and molecular events, including matrix deposition of collagen type I and a large number of extracellular noncollagenous proteins followed by matrix mineralization.[9] Based on this understanding, the osteoblastic phenotype ex vivo has been defined by the ability of cells to express a number of

biomarkers known to be relevant for bone formation, for example, production of alkaline phosphatase (ALP), type I collagen (ColI), osteopontin (OP), bone sialoprotein (BSP), and osteocalcin (OC), as well as the ability to form mineralized matrix ex vivo.[11,12]

In recent years, the commitment of BMSCs to osteoblastic cells has been tested by demonstrating the ability of the cells to form heterotopic bone in vivo when implanted subcutaneously mixed with an osteoconductive material: hydroxyapatite–tricalcium phosphate (HA-TCP) in immune-deficient mice.[13–16] The bone formed provides a better readout of the commitment of BMSCs to osteoblastic lineage and consequently their in vivo behavior.[13–16] However, when clonally derived BMSCs populations were tested in this assay, not all the clonal cells were able to form bone in vivo,[4] and the ex vivo markers of osteoblastic phenotype (e.g., ALP) were not predictive of the in vivo bone-forming capacity.[4] Therefore, it is of a great interest to define ex vivo molecular markers that are better at predicting the in vivo bone-formation capacity of BMSCs.

The availability of large-scale methods for gene profiling using DNA microarrays has encouraged several investigators to define the phenotype of ex vivo cultured cell populations in terms of expression of a large number of genes, that is, "molecular signature," and this method has been employed to characterize BMSCs derived from various sources and during differentiation to osteoblastic cells or other cell lineages.[17–21] Thus the aim of this study was to define an ex vivo molecular phenotype of hBMSCs populations that are committed to osteoblastic lineage, which was defined as the ability to form bone in vivo in heterotopic bone-formation assays. We employed a recently developed hBMSCs cell line stably expressing the human telomerase reverse-transcriptase (*hTERT*) gene (named hBMSC-TERT)[22,23] as a model for human BMSCs, and we compared the whole transcriptome in two cell populations derived from the parental cell line: an in vivo bone-forming (hBMSC-TERT[+Bone]) population and a non-bone-forming hBMSC-TERT[−Bone] population using the Affymetrix DNA Microarray platform (Santa Clara, CA, USA). We verified the molecular signature by testing its association with bone-forming capacity using hBMSCs clonal cell lines with variable capacity for in vivo bone formation.

Material and Methods

Cell culture

The establishment and characterization of the hBMSC-TERT cell line were described previously.[22,23] The hBMSC-TERT[+Bone] cells were derived from early-passage hBMSC-TERT cells [population doubling level (PDL) 77], and the hBMSC-TERT[−Bone] cells were derived from late-passage hBMSC-TERT cells (PDL 233). The cells were cultured in a standard growth medium containing minimal essential medium (MEM) (Gibco Invitrogen, Carlsbad, CA, USA) supplemented with 10% FCS (Biochrom, Berlin, Germany) and 1% penicillin/streptomycin (Gibco Invitrogen) at 37°C in a humidified atmosphere containing 5% CO_2.

Long-term cell growth

Long-term cell growth ex vivo was determined by calculating cumulative PDL. At confluence, the cells were incubated with trypsin/EDTA (Gibco Invitrogen), and cells were counted using a hemocytometer. At each passage, the initial cell number and the number of cells at confluence were determined. Population doubling (PD) was determined using the formula log N/log 2, where N is the number of cells at confluence divided by the initial cell number. Cumulative PDL thus is the sum of population doublings at each passage.

Establishing hBMSC single-cell clones by limiting dilution method

Single-cell clones were establishing by seeding hBMSC-TERT cells in 100 μL of medium at a concentration of 0.3 cell per well in four flat-bottomed 96-well plates. Wells containing only one cell were identified and marked within 12 hours of seeding using an inverted microscope. These wells were monitored subsequently for growth of only a single colony per well. Clones at approximately 60% confluence were trypsinized and passaged into 24-well plates. A clonal cell line was considered established when the cells were able to undergo at least 20 PD (>10^6 cells). Six clones with different bone-forming abilities were employed for this study.

Short-term proliferation rate

The six selected clones and the parental hBMSC-TERT population were seeded in 24-well plates (Nunc, Roskilde, Denmark) at a density of 4000 cells/cm². Cell proliferation was monitored by harvesting cells in triplicate and counting using a hemocytometer on days 1, 3, 6, 9, 12, and 15. The average and standard error of the mean (SEM) from the triplicate counts were calculated, plotting values for each sample into a graph.

Ex vivo cell differentiation studies

Osteoblast differentiation

Cells were plated at a density of 6250 cells/cm² in 6-well plates in standard growth medium. At 70% to 80% confluence, the medium was replaced with osteogenic medium consisting of minimum essential medium (MEM) + 10% fetal calf serum (FCS) and 1% penicillin/streptomycin supplemented with 10 mM β-glycerophosphate (Calbiochem, La Jolla, CA, USA), 50 μg/mL L-ascorbic acid (Wako Chemicals GmbH, Neuss, Germany), 10 nM dexamethasone (Sigma Chemical Co., St. Louis, MO, USA), and 10 nM calcitriol (1,25-dihydroxyvitamin D_3; kindly provided by Leo Pharma, Ballerup, Denmark). The medium was replaced every 3 days. The control cells were grown in standard growth medium. Cell pellets were harvested for RNA isolation at 0, 7, 14, and 21 days after induction. At day 21, cells were stained for mineral deposition (see below).

Total RNA extraction and real-time reverse-transcriptase polymerase chain reaction (RT-PCR)

Total cellular RNA was isolated using a single-step method with TRIzol (Invitrogen, Taastrup, Denmark) according to the manufacturer's instructions. First-strand complementary cDNA was synthesized from 4 μg of total RNA using a revertAid H minus first-strand cDNA synthesis kit (Fermentas, St. Leon-Rot, Germany) according to the manual instructions.

Real-time PCR was performed using the iCycler IQ detection system (Bio-Rad, Hercules, CA, USA) and SYBR Green I as a double-strand DNA–specific binding dye. Thermocycling was performed in a final volume of 20 μL containing 3 μL of cDNA sample (diluted 1:20), 20 pmol of each primer, and 2× iQ SYBR Green Supermix (Bio-Rad). The quantification of gene expression for each target gene and reference gene was performed in separate tubes using primers as shown in Supplementary Table 1. We used a denaturing step at 95°C for 3 minutes and 40 cycles of 95°C for 30 seconds, 60°C for 30 seconds, and 72°C for 1 minute. Each reaction was run in duplicate, and fluorescence data were collected at the end of the extension step in every cycle. To ensure specific amplification, a melting curve was calculated for each PCR reaction by increasing the temperature from 60 to 95°C with a temperature increment rate of 0.5°C/10 seconds. Fold induction and expression levels for each target gene were calculated using the comparative C_T method [i.e., $1/(2^{\Delta C_T})$, where ΔC_T is the difference between C_T target and C_T reference] after normalization to β-actin mRNA (PerkinElmer's User Bulletin No. 2), and data were analyzed using optical system software Version 3.1 (Bio-Rad) and Microsoft Excel 2000 to generate relative expression values.

Cytochemical staining

Alizarin red S (AR-S) staining

Assessment of ex vivo mineralization was performed employing alizarin red S (AR-S) staining. Cells were induced into osteoblast differentiation as described earlier for 21 days. The cells were washed in PBS, fixed in 70% ethanol at −20°C for 1 hour, and rinsed in dH_2O. The cultures were stained with 40 mM AR-S (Sigma-Aldrich, St. Louis, MO, USA), pH 4.2, for 10 minutes with rotation. Cells then were rinsed twice with dH_2O, followed by washing three times with PBS to reduce nonspecific staining.

Alkaline phosphatase (ALP) activity assay

Cells were cultured in 24-well plates at 20×10^3 cells/cm². At 80% confluence, cells were induced to differentiate into osteoblasts using the previously mentioned osteoblastic-induction medium. Colorimetric ALP activity assay on whole-cell extracts was performed using p-nitrophenyl phosphate as a substrate (ABX Pentra ALP CP kit, HORIBA ABX Diagnostics, Northampton, UK). ALP activity was normalized to total cellular protein assessed by the Bradford assay (Bio-Rad) and expressed as units per milligram of protein. One unit of ALP activity is defined as the enzyme activity that will liberate 1 μM of p-nitrophenol per 30 minutes at 37°C.

In vivo bone-formation assay in immunodeficient mice

Cells (5×10^5) mixed with hydroxyapatite–tricalcium phosphate ceramic powder (HA-TCP, 40 mg; Zimmer Scandinavia, Albertslund, Denmark) were transplanted subcutaneously into the dorsal surface of 8-week-old female NOD/SCID mice (NOD/LtSz-Prkd^{cscid}), as described previously.[13,16] The implants were recovered after 8 weeks and transferred to 4% neutral buffered formalin for about 45 minutes; afterwards, formic acid was added for 2 days. Using standard histopathologic methods, the HA-TCP implants were embedded in paraffin, and tissue sections (4 μm thick) were cut and stained with hematoxylin and eosin Y (Bie & Berntsens Reagenslaboratorium, Herlev, Denmark) using standard methods. The total bone volume per total volume was quantified as described previously.[13,24]

DNA microarray analysis

Both hBMSC-TERT^{+Bone} and hBMSC-TERT^{-Bone} populations were cultured in triplicate at 3×10^4 cells/cm² in Petri dishes in standard growth medium. At 90% to 100% confluence, highly purified total cellular RNA was isolated from each of three independent cultures per cell line using an RNeasy Kit (QIAGEN, Valencia, CA, USA) according to the manufacturer's instructions. First- and second-strand cDNA syntheses were performed from 8 μg total RNA using the SuperScript Choice System (Life-Technologies, Carlsbad, CA, USA) according to the manufacturer's instructions. Subsequent hybridization and scanning of the Affymetrix GeneChip arrays were performed as described previously.[25] The biotinylated targets were hybridized to U133 Plus 2.0 Array Affymetrix GeneChip oligonucleotide arrays. Expression measures were generated and normalized using the RMA procedure[26] implemented in the Bioconductor package (www.bioconductor.org/). Values were $\log_2$ transformed and imported into Microsoft Excel. Before analyzing the expression data from the U133 Plus 2.0 Array, Affymetrix control probes were removed.

Flow cytometric (FACS) analysis

Cells were cultured in standard growth medium to 90% confluence, trypsinized, and washed twice in FACS buffer [PBS containing 0.5% BSA (Sigma), 25 nM EDTA (Sigma)]. The cells were stained with specific conjugated primary antibodies for 15 minutes at 4°C. Afterwards, samples were washed twice with FACS buffer and analyzed by FACScan flow cytometer (Becton-Dickinson, San Jose, CA, USA) linked with Cell-Quest 3.1 software (Becton-Dickinson). A list of the antibodies used is provided in Supplementary Table 2.

Statistic analysis

For the microarray analysis, a two-tailed t test was applied to analyze the differentially expressed genes between the two groups, and a p value of .001 was used as threshold for statistical significance. From the group of significantly changed genes, we selected genes that exhibited more than fourfold change for further analysis. Correlation between variables was determined using Pearson's correlation, and differences between groups were examined by two-tailed t test, and a p value of less than .05 was considered statistically significant.

Results

Characterization of hBMSC-TERT^{+Bone} and hBMSC-TERT^{-Bone}

As shown in Fig. 1, both hBMSC-TERT^{+Bone} and hBMSC-TERT^{-Bone} populations are derived from the parental hBMSC-TERT cell line[23] at different PDLs (see Fig. 1A,B). When the cells were implanted

mixed with HA-TCP subcutaneously in immune-deficient mice, only hBMSC-TERT^{+Bone} formed bone tissue (see Fig. 1C). We have demonstrated previously that the bone formed was derived from the donor cells using human-specific ColI, OC, and OP antibodies.[13,23] Interestingly, despite the different ability of these cell populations for in vivo bone formation (see Fig. 1C), both cell populations expressed ex vivo osteoblastic markers ALP, ColI, and OC (see Fig. 1D) and were able to form ex vivo mineralized matrix visualized by alizarin red staining (see Fig. 1E). We performed a FACS analysis of known surface markers of BMSCs[1,5] in hBMSC-TERT^{+Bone} and hBMSC-TERT^{-Bone} populations. Both cell lines exhibited similar levels of standard surface markers of BMSCs: CD63 (100%), CD73 (100%), CD105 (100%), and CD166 (100%) (Supplementary Fig. 1A, B). Interestingly, CD146^{+} cells were few among hBMSC-TERT^{-Bone} cells compared with hBMSC-TERT^{+Bone} cells (2% versus 79%, respectively). Similarly, quantitative PCR analysis demonstrated a 37-fold downregulation of CD146 gene expression in hBMSC-TERT^{-Bone} cells compared with its expression levels in hBMSC-TERT^{+Bone} cells (see Supplementary Fig. 1C).

Identification of genes associated with in vivo bone formation using DNA microarray

We compared the whole transcriptome of hBMSC-TERT^{+Bone} and hBMSC-TERT^{-Bone} to identify the molecular phenotype predictive of in vivo bone formation using the Affymetrix DNA microarrays platform. The number of genes that changed significantly for each group was relatively small compared with the total number of genes interrogated (~47,000). For hBMSC-TERT^{+Bone}, 168 genes were significantly upregulated, and for hBMSC-TERT^{-Bone}, 197 genes were significantly upregulated. In order to verify the observed changes, we employed real-time PCR analysis. We studied the expression profile of 24 genes that showed the most significant changes in hBMSC-TERT^{+Bone} and hBMSC-TERT^{-Bone} cells under basal culture conditions. As shown in Supplementary Fig. 2, quantitative PCR analysis confirmed the changes revealed by the DNA microarray data.

Functional classification of the differentially regulated genes

To investigate the major differences between the hBMSC-TERT^{+Bone} and hBMSC-TERT^{-Bone} cells in more detail, we employed the Web tool fatiGO+[27] to classify the genes according to gene ontology and transcription factor–binding sites (Table 1). Interestingly, we found that the main difference between the significantly upregulated genes in hBMSC-TERT^{+Bone} cells compared with hBMSC-TERT^{-Bone} cells was an
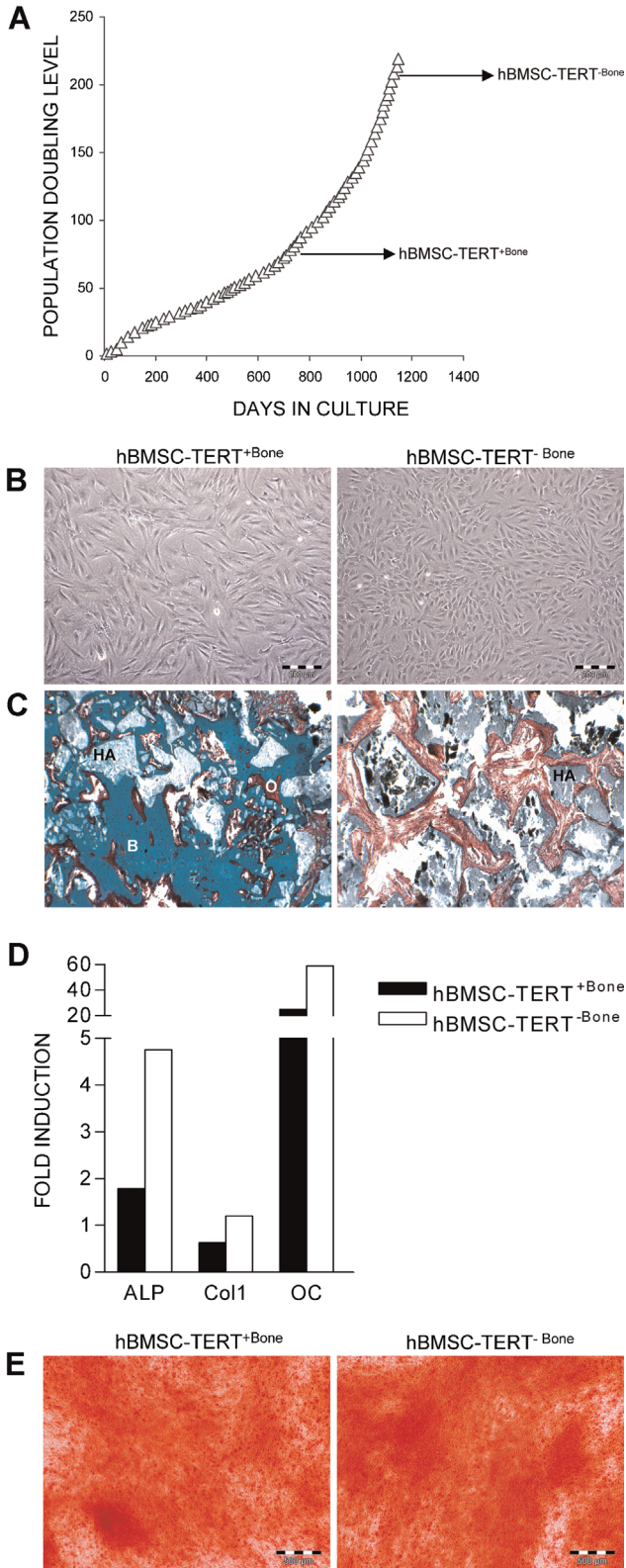

Fig. 1. (A) Long-term growth curve of human bone marrow stromal cells (hBMSCs) overexpressing telomerase reverse-transcriptase gene (hBMSC-TERT). The arrows denote the population doubling levels where bone-forming hBMSC-TERT^{+Bone} and non-bone-forming: hBMSC-TERT^{-Bone} populations were derived. (B) Ex vivo culture morphology of hBMSC-TERT^{+Bone} and hBMSC-TERT^{-Bone} cells. (C) In vivo bone-formation assay was performed by implanting the cells mixed with hydroxyapatite–tricalcium phosphate (HA-TCP) subcutaneously into immune-deficient mice for 8 weeks. Plastic-embedded sections were stained with Goldner's trichrome. B = bone; O = osteoid; HA = hydroxyapatite–tricalcium phosphate. Only hBMSC-TERT^{+Bone} and not hBMSC-TERT^{-Bone} cells formed bone in vivo. (D) Effects of ex vivo osteoblastic differentiation induction (day 12) on gene expression of a selective group of canonical osteoblastic markers: alkaline phosphatase (ALP), collagen type 1 (Col1), and osteocalcin (OC) in hBMSC-TERT^{+Bone} and hBMSC-TERT^{-Bone} cells. (E) Ex vivo mineralization capacity visualized by alizarin red staining in hBMSC-TERT^{+Bone} and hBMSC-TERT^{-Bone} cells 21 days after induction of osteoblast differentiation.

MOLECULAR PHENOTYPE OF OSTEOGENIC STEM CELLS

Journal of Bone and Mineral Research   799 ■

Table 1. Distribution (%) of Extracellular Matrix (ECM), Immune-Response-Related Genes and Genes Having SP3-Binding Sites in Their Promoter Region (SP3) in Bone-Forming (hBMSC-TERT^{+Bone}) and Non-Bone-Forming (hBMSC-TERT^{-Bone}) Mesenchymal Stem Cell Lines

Gene category	hBMSC-TERT^{+Bone}	hBMSC-TERT^{-Bone}
Extracellular matrix	17	5
Immune-response-related	8	26
SP3	21	8

overrepresentation of extracellular matrix (ECM) and skeletal development genes. On the other hand, hBMSC-TERT^{-Bone} cells expressed a larger number of immune-response-related genes (see Table 1). We also found that genes expressed in hBMSC-TERT^{+Bone} cells had a higher occurrence of potential SP3 transcription factor–binding sites in their promoter region compared with hBMSC-TERT^{-Bone} cells (21% versus 8%, respectively). Sp3 is a broadly expressed transcription factor and is essential for appropriate skeletal ossification and maturation during bone development. Endochondral and intramembranous ossifications are impaired in Sp3-deficient mouse embryos.[28]

Extracellular matrix (ECM) genes

Most of the significantly upregulated genes (>5-fold, $p < .0001$) in hBMSC-TERT^{+Bone} cells were annotated as ECM and included a large group of genes involved in bone matrix assembly (Table 2A). Among these, we identified *DCN* (decorin), *MFAP2* (microfibrillar-associated protein 2), *BGN* (biglycan), *LUM* (lumican), and *LOXL4* (lysyl oxidase-like 4). In addition to these well-known bone matrix genes, we have identified two muscle-related genes: *SGCD* (δ-sarcoglycan) and *SGCE* (ε-sarcoglycan). They are part of a multimeric complex (including, in addition, α-, β-, and γ-sarcoglycan) that associates with dystrophin, dystroglycan, and other proteins to constitute the larger dystrophin-glycoprotein complex at the muscle membrane of both skeletal and cardiac muscle.[29,30]

Skeletal development genes

A subset of genes known to be important in skeletal development was exclusively upregulated in hBMSC-TERT^{+Bone} cells (see Table 2B), including *CLEC3B* (tetranectin), *NPR3* (natriuretic peptide receptor C), *TNFRSF11B* (tumor necrosis factor receptor superfamily member 11b), *DLX5* (distal-less homeo box 5), and *POSTN* (periostin).

Immune-related genes

Impaired in vivo bone formation in hBMSC-TERT^{-Bone} cells was associated with significant upregulation of a large number of immune-regulatory factors (>4-fold, $p < .0001$), including several chemokines: *CXCL2* [chemokine (C-X-C motif) ligand 2], *IL8* (interleukin 8), *CXCL11* [chemokine (C-X-C motif) ligand 11], and

immune response-related genes *BST2* (bone marrow stromal cell antigen 2), *CD24* [CD24 antigen (small cell lung carcinoma cluster 4 antigen)], and *TNFRSF11A* (tumor necrosis factor receptor superfamily member 11a), also named *RANK*, which is known to activate the NF-κB signaling pathway[31] (see Table 2C).

Examining the ability of the ex vivo expression of novel molecular markers to predict hBMSCs in vivo bone formation

The preceding results suggest the presence of a number of molecular markers associated with osteoblastic lineage commitment, as evidenced by bone-formation capacity in vivo, and thus define an ex vivo phenotype of bona fida osteogenic BMSCs. In order to confirm the predictive value of this molecular signature and to compare the novel molecular markers with the canonical osteoblastic markers, we examined the ex vivo gene expression of these genes in hBMSC-TERT-derived clonal cell lines with varying in vivo bone-forming capacity.

We established 118 single-cell clones, and six of these clones were chosen for more extensive analysis based on the presence of uniform and distinct morphology (Fig. 2A). The clones were named DD8, AD10, BB10, CF1, CB4, and CD8 (see Fig. 2A). The clones AD10, BB10, and DD8 displayed a long, thin rectangular shape and a degree of contact inhibition. The CB4 clone had a fusiform spindle-like morphology, and CD8 and CF1 formed clustered of cuboidal cells (see Fig. 2A).

On subcutaneous implantation into immune-deficient mice, the clones formed a variable amount of heterotopic bone (see Fig. 2B, C). We classified the clones into high-bone-forming (HBF) clones—DD8, AD10, and BB10—and low-bone-forming (LBF) clones—CD8, CB4, and CF1—based on the amount of bone formed compared with the parental hBMSC-TERT cell line (see Fig. 2C).

We examined the ex vivo phenotype of these clones to identify predictive markers for the in vivo bone-forming capacity. The short-term proliferation rates of the six selected clones and the parental hBMSC-TERT cell line are shown in Fig. 3A. Significant differences in growth rates were apparent between days 3 and 9. CF1 had the fastest growth rate, followed by the CB4 and CD8 clones. Interestingly, HBF clones exhibited a slower growth rate than the LBF clones (see Fig. 3A).

FACS analysis of standard BMSC surface markers demonstrated that both HBF clones (e.g., DD8) and LBF clones (e.g., CF1) exhibited a similar percentage of cells positive for CD63 (100%), CD73 (100%), CD105 (100%), and CD166 (100%). Also, the number of CD146$^+$ cells was similar in DD8 (85%) and CF1 (82%) clones (see Supplementary Fig. 1A, B), and both clones exhibited similar gene expression levels of CD146 (see Supplementary Fig. 1C).

Figure 3B, C demonstrates the ex vivo osteoblastic differentiation capacity of the six cell clones as well as the parental hBMSC-TERT cell line. We found a discrepancy between in vivo bone-forming capacity and the ex vivo mineralization assay. The CF1 clone (an LBF clone) and the parental hBMSC-TERT cell lines formed extensive ex vivo mineralized matrix stained by alizarin red, whereas the HBF clones did not exhibit enhanced ex vivo mineralization (see Fig. 3B). Similarly, the CF1 and CB4 clones

Table 2. Genes Differentially Upregulated in Bone-Forming Human Bone Marrow Stromal Cells: hBMSC-TERT^{+Bone} Versus Non-Bone-Forming hBMSC-TERT^{-Bone} Cell Lines

Affymetrix probe set ID	Gene title	Gene symbol	Fold change	p Value
A: Genes Involved in Extracellular Matrix Upregulated in hBMSC-TERT^{+Bone} Compared with hBMSC-TERT^{-Bone}				
213765_at	Microfibrillar associated protein 5	MFAP5	41.3	1.89E-05
231879_at	Collagen, type XII, alpha 1	COL12A1	20.9	2.24E-04
229554_at	Lumican	LUM	15.6	1.53E-04
203417_at	Microfibrillar-associated protein 2	MFAP2	13.1	9.90E-05
212670_at	Elastin (supravalvular aortic stenosis, Williams-Beuren syndrome)	ELN	10.9	2.38E-05
242605_at	Decorin	DCN	5.8	1.98E-04
214492_at	Sarcoglycan, δ (35-kDa dystrophin-associated glycoprotein)	SGCD	5.3	2.89E-04
204298_s_at	Lysyl oxidase	LOX	5.1	3.06E-04
225681_at	Collagen triple helix repeat containing 1	CTHRC1	5.0	2.28E-04
222486_s_at	A disintegrin-like and metalloprotease (reprolysin type) with thrombospondin type 1 motif 1	ADAMTS1	4.9	3.06E-04
204688_at	Sarcoglycan, ε	SGCE	4.7	3.08E-04
201843_s_at	EGF-containing fibulin-like extracellular matrix protein 1	EFEMP1	4.2	8.39E-05
B: Genes Involved in Skeletal Development Upregulated in hBMSC-TERT^{+Bone} Compared with hBMSC-TERT^{-Bone}				
205200_at	C-type lectin domain family 3, member B	CLEC3B	50.1	8.93E-06
219789_at	Natriuretic peptide receptor C/guanylate cyclase C	NPR3	27.0	1.70E-04
231879_at	Collagen, type XIIα1	COL12A1	20.9	2.23E-04
204933_s_at	Tumor necrosis factor receptor superfamily member 11b	TNFRSF11B	9.4	2.41E-05
213707_s_at	Distal-less homeobox 5	DLX5	4.5	1.40E-04
1555778_a_at	Periostin, osteoblast-specific factor	POSTN	3.9	4.79E-05
C: Immune-Response Genes Upregulated in hBMSC-TERT^{-Bone} Compared with Bone-Forming hBMSC-TERT^{+Bone}				
202411_at	Interferon-α-inducible protein 27	IFI27	59.6	1.86E-05
202086_at	Myxovirus (influenza virus) resistance 1 interferon-inducible protein p78 (mouse)	MX1	30.2	2.91E-04
205552_s_at	2′,5′-Oligoadenylate synthetase 1, 40–46 kDa	OAS1	24.7	7.11E-05
201641_at	Bone marrow stromal cell antigen 2	BST2	20.8	2.03E-04
201288_at	Rho GDP dissociation inhibitor (GDI) β	ARHGDIB	19.8	6.90E-04
202859_x_at	Interleukin 8	IL8	18.8	2.78E-04
225647_s_at	Cathepsin C	CTSC	18.6	3.49E-05

Table 2. (*Continued*)

Affymetrix probe set ID	Gene title	Gene symbol	Fold change	*p* Value
205483_s_at	Interferon-α-inducible protein (clone IFI-15K)	G1P2	13.4	1.58E-06
222838_at	SLAM family member 7	SLAMF7	12.2	6.63E-04
210029_at	Indoleamine-pyrrole-2,3-dioxygenase	INDO	11.4	1.90E-04
218400_at	2′-5′-Oligoadenylate synthetase 3, 100 kDa	OAS3	11.2	4.25E-04
266_s_at	CD24 antigen (small cell lung carcinoma cluster 4 antigen)	CD24	10.8	8.22E-05
204994_at	Myxovirus (influenza virus) resistance 2 (mouse)	MX2	10.4	6.39E-04
227458_at	CD274 antigen	PDCD1LG1	10.3	5.59E-05
203153_at	Interferon-induced protein with tetratricopeptide repeats 1	IFIT1	8.5	3.80E-05
204747_at	Interferon-induced protein with tetratricopeptide repeats 3	IFIT3	8.4	1.96E-05
234987_at	SAM domain and HD domain 1	SAMHD1	8.4	3.42E-05
205660_at	2′-5′-Oligoadenylate synthetase-like	OASL	7.2	7.57E-05
209774_x_at	Chemokine (C-X-C motif) ligand 2	CXCL2	6.1	9.59E-04
238846_at	Tumor necrosis factor receptor superfamily member 11a activator of NF-κB	TNFRSF11A	5.4	2.89E-05
211122_s_at	Chemokine (C-X-C motif) ligand 11	CXCL11	4.7	2.55E-05
205891_at	Adenosine A2b receptor	ADORA2B	4.2	3.30E-06
202270_at	Guanylate binding protein 1, interferon-inducible, 67 kDa	GBP1	4.2	2.66E-04

Note: The basal gene expression profile of hBMSC-TERT^{+Bone} versus hBMSC-TERT^{-Bone} was determined using Affymetrix DNA microarrays. A total of 168 genes were significantly upregulated in hBMSC-TERT^{+Bone}. Gene annotation based on biologic process and molecular function revealed overrepresentation of extracellular matrix (ECM) genes (*A*) and skeletal development genes (*B*) in hBMSC-TERT^{+Bone}, whereas hBMSC-TERT^{-Bone} displayed high expression of immune-response-related genes (*C*).

(both LBF clones) expressed higher levels of ALP activity than all other tested clones (see Fig. 3*C*).

We also determined the baseline expression levels of the canonical osteoblastic marker genes (*CBFA1/Runx2*, *ALP*, *Col1*, *OP*, *OC*, and *BSP*), as well as the novel molecular markers identified in the microarray data, using real-time PCR in both HBF and LBF clones. At baseline, the expression levels of *OC* and *BSP* were very low (threshold value of these markers in real-time PCR assay was > 30). We found no significant positive correlation between the levels of *CBRA1/Runx2*, *ALP*, *Col1*, or *OP* and the ability to form bone in vivo (Table 3 and Fig. 4). Interestingly, several of the genes identified by the DNA microarray were better predictors of the in vivo bone-forming capacity of BMSCs clones. Baseline gene expressions of *DCN*, *NPR3*, *CLECB3*, and to a lesser degree *LOXL4* were significantly higher in HBF clones (DD8, AD10, and BB10) than in LBF clones (CD8, CB4, and CF1) (see Figure 4). Also,

the amount of in vivo formed bone exhibited a positive correlation with the expression levels of these genes across different clones ($r = 0.92$ to 0.98, $p < .01$) (see Table 3). The immune regulatory genes *MX1* and *SLAMF7* were significantly higher in LBF clones than in HBF clones, but the negative correlation between the amount of in vivo bone formed and their basal gene expressions across different clones did not reach statistical significant ($r = -0.78$, $p = -.07$, $r = -0.68$, $p = 0.13$, respectively) (see Table 3).

In order to test the ability of the novel molecular markers to prospectively identify the bone-forming clones, we further screened 10 independent hBMSC-TERT clones and identified three clones that exhibited high expression levels of *Elastin*, *DCN*, *LOXL4*, *NPR3*, and *CLEC3B* and only one clones that exhibited a high expression of the immune response genes *MX1* and *SLAMF7* with concomitant low expression of levels of *Elastin*, *DCN*, *LOXL4*,
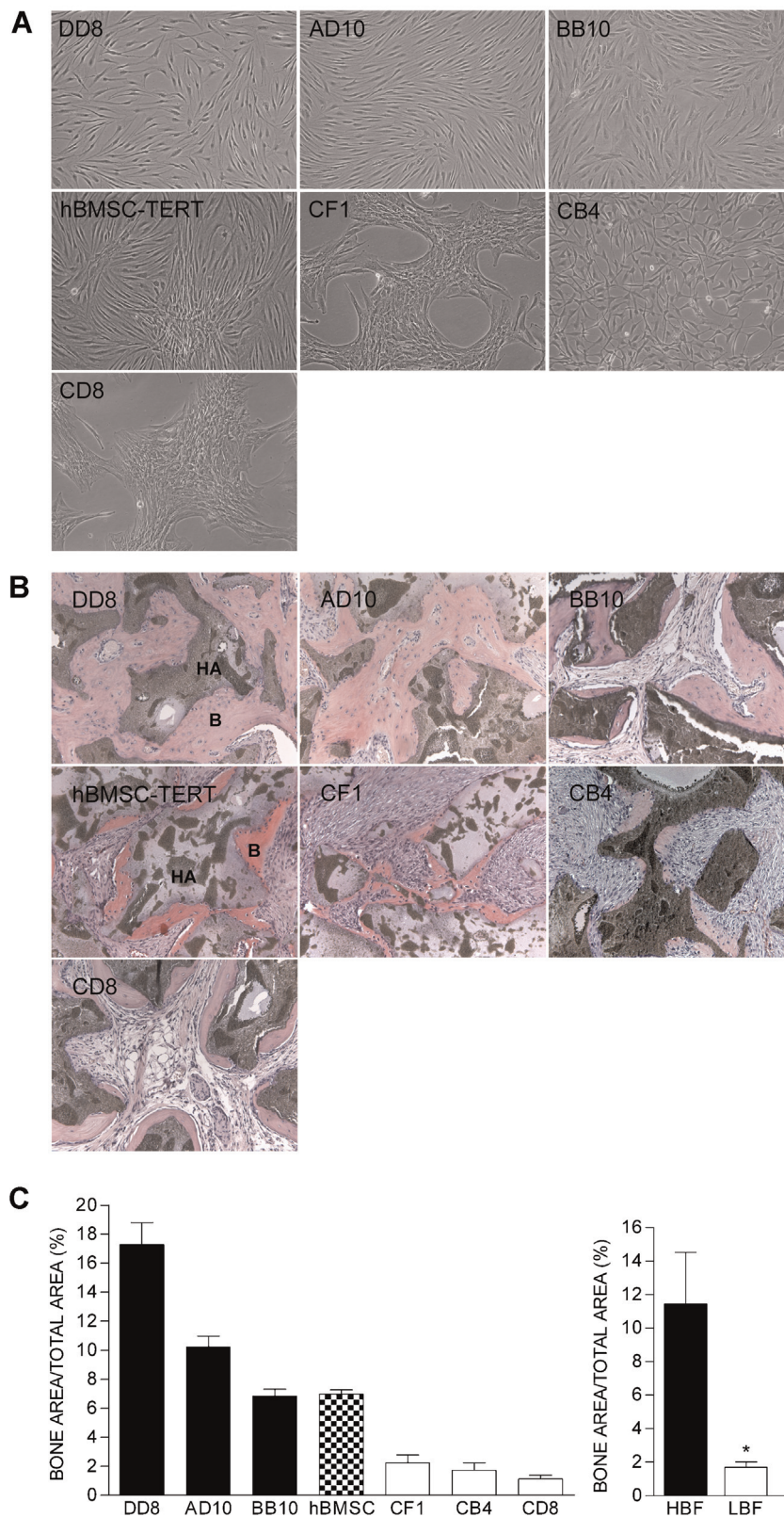
Fig. 2. Clonal heterogeneity in hBMSCs cells. Single-cell clonal cell lines were derived from the hBMSC-TERT population by limiting dilution procedure, and six clones were chosen for more detailed studies. (*A*) Phase-contrast images of the six selected clonal cell lines with different cell morphology. (*B*) Histologic sections showing variable ability for heterotopic bone formation, as demonstrated by implanting different clonal cells with hydroxyapatite–tricalcium phosphate (HA/TCP) subcutaneously into immune-deficient mice for 8 weeks. (*C*) Quantification of the ectopic in vivo bone formed by the six clonal cell lines and the parental hBMSC-TERT cell line. The clonal cell lines were classified as either high-bone-forming (HBF) or low-bone-forming (LBF) cells. *Denotes statistical significance between HBF and LBF.
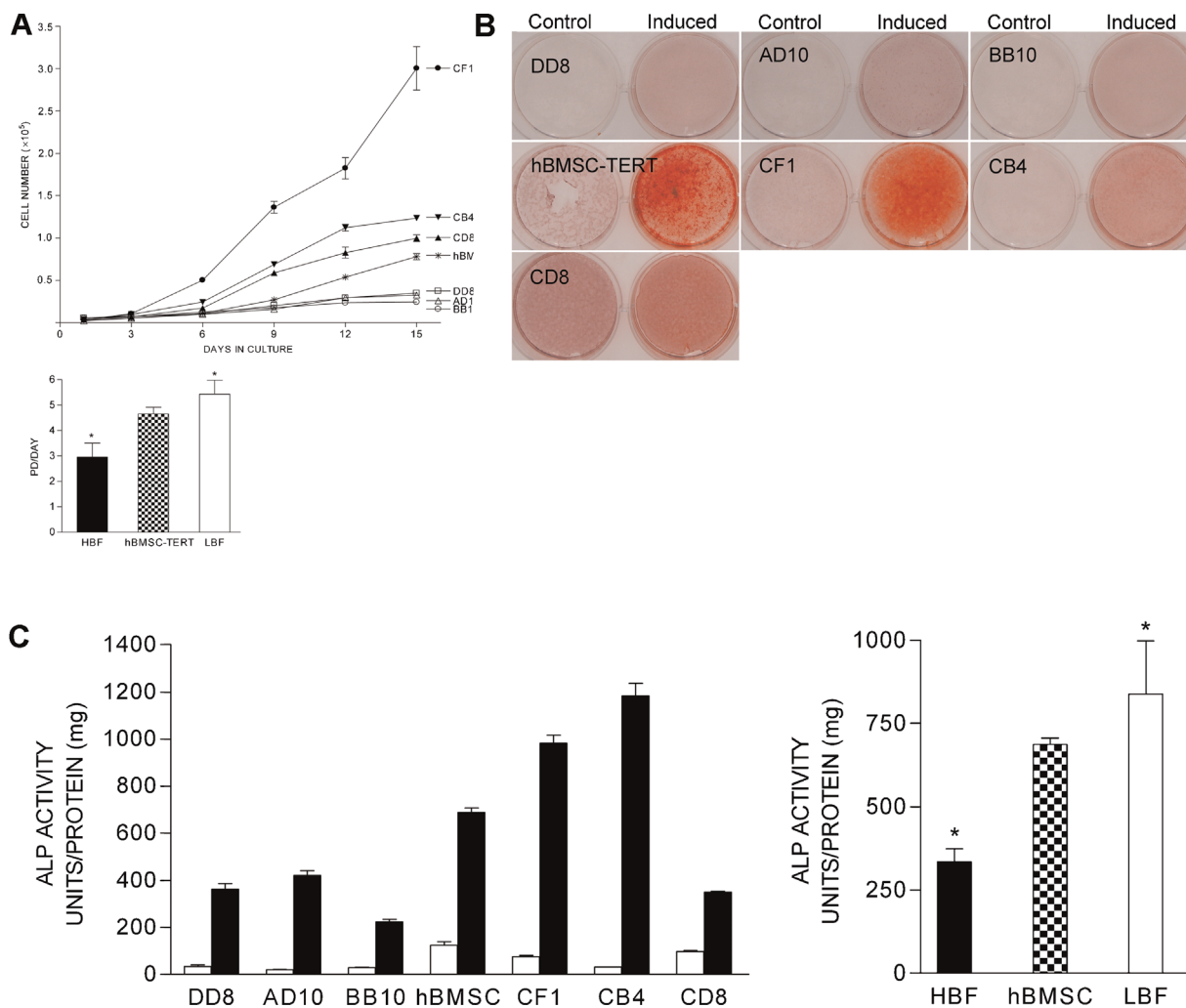
Fig. 3. Ex vivo phenotypic characterization of six hBMSC-TERT clonal cell lines and their parental cell line hBMSC-TERT. The clones are represented in two groups: high-bone-forming (HBF) and low-bone-forming (LBF) based on their ability to form bone in vivo. (A) Short-term growth rate. PD = population doubling. (B) Matrix mineralization as visualized by alizarin red S staining and (C) alkaline phosphatase (ALP) activity measurements in cell extracts at day 21 after ex vivo osteoblast differentiation induction (induced) and compared with control cultures (control). The ALP activity was normalized to the total amount of cellular protein. One unit of ALP activity is defined as the enzyme activity that will liberate 1 μM of p-nitrophenol per 30 minutes at 37°C. *Denotes statistical significance between HBF and LBF.

NPR3, and *CLEC3B*. These clones were tested for their bone-forming capacity by transplantation in vivo. The relationship between the expression levels of these markers and the in vivo bone formed is shown in Supplementary Fig. 1D. As expected, the clones that expressed high levels of *Elastin*, *DCN*, *LOXL4*, *NPR3*, and *CLEC3B* formed more bone in vivo than the clone that exhibited a high expression of the immune response genes *MX1* and *SLAMF7* (see Supplementary Fig. 1E).

Discussion

In this study, we subjected two hBMSCs cell populations that are either bone forming or non–bone forming on in vivo transplantation to global DNA microarray analysis in order to identify a molecular signature predictive of an in vivo bone-formation phenotype. We examined the ability of these characteristics to predict the in vivo bone-forming capacity of BMSCs in an independent nested case-control study employing six different hBMSC-derived single-cell clones with low and high in vivo bone-forming capacity and in four other independent clones isolated prospectively based on the same molecular signature. We identified a number of extracellular matrix genes, skeletal development genes, and immune response genes that were predictive for the ability of cells to form bone in vivo.

Several ECM genes were upregulated in hBMSC-TERT[+Bone]. Biglycan (BGN) and decorin (DCN) are highly enriched in bone extracellular matrix and are capable of binding to transforming growth factor β (TGF-β) and collagen type 1 in the pericellular microenvironment.[32] While *DCN* knockout mice exhibit a normal bone phenotype, *BGN* knockout mice have low bone mass, and *DCN/BGN* double-knockout mice exhibit a more severe bone phenotype, suggesting the importance of both factors for normal bone formation.[33] Microfibrillar-associated protein 2 (MFAP2) is a component of elastin-associated microfibrils that forms a ternary complex with biglycan and decorin.[34,35]

LARSEN ET AL.

Table 3. Correlation of Baseline Gene Expression Levels With the Amount of Bone Formed In Vivo in Clonal hBMSCs Lines

Category	Gene	r Value	p Value
Osteoblastic markers	CBFA1	−0.64	n.s
	ALP	−0.54	n.s
	COL1	−0.53	n.s
	OS	−0.62	n.s
Extracellular matrix genes	Elastin	0.57	n.s
	DCN	0.92	<.01
	LOXL4	0.98	<.001
Skeletal development genes	NPR3	0.94	<.01
	CLEC3B	0.98	<.001
Immune-response-related genes	MX1	−0.78	n.s (.07)
	SLAMF7	−0.68	n.s (.13)

Note: Gene expression levels of several osteoblast molecular markers were determined in six human bone marrow stromal cell (hBMSC) clonal cell lines and correlated with the amount of bone formed by the cells when implanted in vivo subcutaneously for 8 weeks in immune-deficient mice. n.s. = statistically not significant.

Lumican (LUM) belongs to the small leucine-rich proteoglycan family and plays an essential role in regulation of collagen fibril formation in bone matrix.[36,37] Lysyl oxidase-like 4 (LOXL4) belongs to the lysyl oxidase family and is essential for catalyzing the first step of lysine- and hydroxylysine-derived cross-linking of the collagen molecules, as well as lysine-derived cross-linking in elastins. Lysyl oxidase-like 4 is important for collagen assembly by osteoblastic cells.[38,39]

Two muscle-related sarcoglycan genes, *SGCD* (δ-sarcoglycan) and *SGCE* (ε-sarcoglycan), were upregulated in hBMSC-TERT[+Bone]

cells. Sarcoglycans were identified originally in muscle for their involvement in limb-girdle muscular dystrophies, and mice deficient in the *SGCD* gene develop cardiomyopathy and muscular dystrophy. The expression of the muscle-related proteins SGCD and SGCE in hBMSC-TERT[+Bone] cells may suggest a potential of the cells for myogenic differentiation. However, BMSCs do not differentiate spontaneously into myogenic lineage, and this differentiation induction requires treatment with chromatin remodeling agents.[40] Thus the biologic significance of the presence of muscle-related genes in hBMSCs remains to be determined.

Among the group of genes known to be important in skeletal development, *CLEC3B* (tetranectin) was upregulated the most (>50-fold). Tetranectin is an ECM protein involved in proteolysis during tissue remodeling, but its exact function is not known. In the newborn mouse, it is expressed in newly formed woven bone along the periosteum and in the area that becomes the future marrow space.[41] Ex vivo, it is expressed by osteoblastic cells during matrix mineralization in a pattern similar to that of the late bone differentiation markers (e.g., bone sialoprotein), and its overexpression in osteoblastic cells is associated with enhanced in vivo bone formation.[41] The natriuretic peptide receptor C/atrial natriuretic peptide clearance receptor (NPR3) protein is a clearance/decoy receptor with a short cytoplasmic tail, whereas the other two members of this receptor family, natriuretic peptide receptor A and B, are membrane-bound guanylyl cyclases.[42] Mice deficient in NPR3 exhibit a distinct skeletal phenotype including bone overgrowth and increased bone turnover.[43] These effects are assumed to be mediated through changes in the activities of the locally produced natriuretic peptides.[44] The effect of natriuretic peptides on osteoblasts has been shown in osteoblastic cells isolated from rat calvariae. Both atrial natriuretic peptide (ANP) and C-type natriuretic peptide (CNP) increased ex vivo mineralization and the expression of such differentiation markers as alkaline phosphatase.[45] Tumor necrosis factor receptor superfamily member 11B (TNFRSF11B),
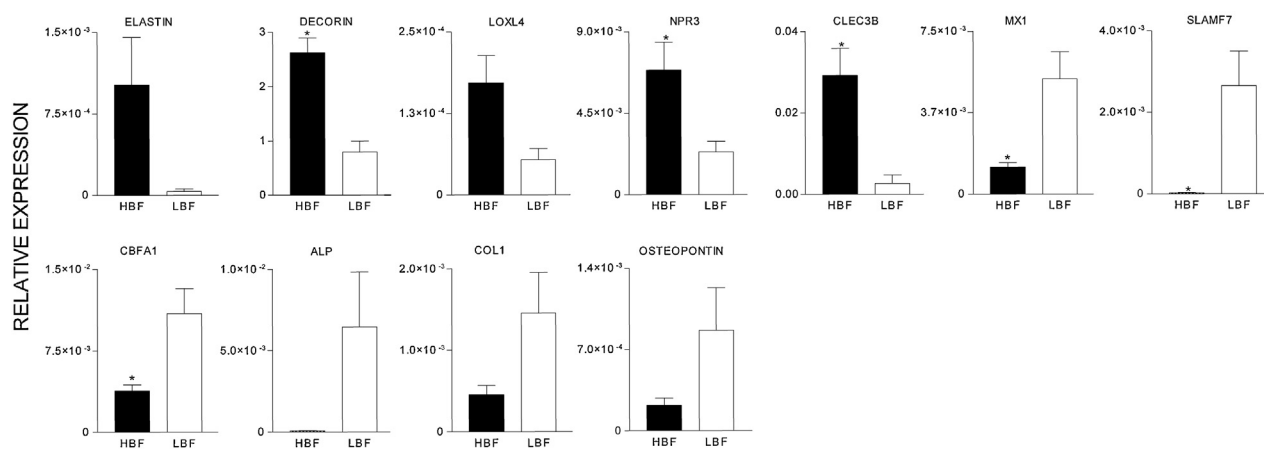

Fig. 4. Gene expression analysis using real-time PCR of a group of differentially regulated genes identified using DNA microarray and a selected group of canonical osteoblastic markers in six hBMSC-TERT clonal cell lines and their parental cell line hBMSC-TERT. The clones are represented in two groups: high-bone-forming (HBF) and low-bone-forming (LBF) based on their ability to form bone in vivo. Lysyl oxidase-like 4 (*LOXL4*), natriuretic peptide receptor C (*NPR3*), tetranectin (*CLEC3B*), myxovirus resistance 1 (*MX1*), SLAM family member 7 (*SLAMF7*), alkaline phosphates (*ALP*), and collagen type I (*Col1*). *Denotes statistical significance between HBF and LBF.

also known as *osteoprotegerin* (OPG), is a member of the TNF-receptor superfamily and functions as an osteoblast-secreted decoy receptor that inhibits bone resorption through binding to RANKL (TNFSF11/OPGL), which is a key extracellular regulator of osteoclast differentiation and function.[46] Distal-less homeobox 5 (DLX5) is a member of the homeobox transcription factor family similar to the *Drosophila* distal-fewer protein. It plays an important role in skeletal development[47] and binds to the homeodomain-response elements in the *RUNX2* gene distal promoter.[48] Periostin (POSTN) is a secreted cell adhesion protein that has been suggested to support osteoblastic cell attachment and spreading.[49] Periostin has been shown to be a ligand for α-integrins promoting integrin-dependent cell adhesion and motility.[50] Periostin is produced by osteoblastic cells,[50,51] and periostin-deficient mouse exhibits dwarfism, decreased bone mass, and an early-onset periodontal disease–like phenotype.[52] Recently, carboxylated periostin has been shown to be localized in the mineralized nodules formed by BMSCs ex vivo, suggesting a role in ECM mineralization.[53]

Loss of the ability to form bone in vivo in hBMSC-TERT[−Bone] cells was associated with an upregulation of a large number of immune-response genes. Stimulation of immune-response pathways including NF-κB has been shown to inhibit osteoblast differentiation and induce bone resorption in many bone inflammatory diseases such as arthritis and periodontal disease.[54] Interestingly, a large number of the immune-response-related genes presented in Table 2*C* are interferon-inducible (e.g., *IFI27*, *GBP1*, and *OAS1*). Several previous studies have demonstrated that interferon-γ enhances osteoclastic bone resorption and exerts inhibitory effects on bone formation.[55,56] Other studies also have revealed that activated T cells inhibit osteoclastogenesis through interferon-γ production.[57] Our study suggests that cell autonomous activation of the interferon signaling pathway leads to impaired bone-formation capacity possibly owing to production of several proinflammatory cytokines with negative effects on bone formation in the pericellular environment. Alternatively, the non-bone-forming populations of BMSCs represent an "osteoblastic" cell population with immune regulatory and proinflammatory roles rather than bone formation. It is also possible that this cell population is expanded during inflammatory conditions associated with bone loss. This hypothesis needs further studies for verification.

We found that baseline measurements of the gene expression of canonical osteoblastic markers, for example, *ALP*, *CBFA1*, *OP*, *Col1*, *BSP*, and *OC*, were not able to predict osteogenic BMSCs populations. Also, both hBMSC-TERT[+Bone] and hBMSC-TERT[−Bone] cells fulfilled definition criteria of BMSCs being CD63^{+}CD73^{+}CD105^{+}CD166^{+} and CD45^{−}CD34^{−}, thus removing the possibility of the presence of non-BMSC contamination. Our data suggest that measuring in vitro differentiation markers can be artefactual, which may be caused by a number of factors. The canonical osteoblastic markers may be specific for the osteoblastic commitment phenotype in general but lack the sensitivity to detect in vivo bone-formation capacity, which requires additional cellular characteristics, including the ability to produce a large number of ECM proteins, as identified in our data. It is also plausible that the osteoblastic phenotype is complex and involves a number of functional subpopulations,

only some of which are concerned with bone formation, whereas others perform other functions (e.g., immune modulation or hematopoiesis support). Thus the canonical osteoblastic markers define the "minimal criteria" for commitment of a cell to the osteoblastic phenotype without distinction among functional subpopulations.[1] In this context, our findings concerning CD146 can be explained. Surface expression of CD146 distinguished between bone-forming and non-bone-forming hBMSCs and thus corroborates the recent data of Sacchetti and colleagues.[58] However, CD146 expression did not correlate with bone-forming capacity, suggesting that it is necessary but not sufficient for defining the in vivo bone-forming BMSCs population. The data provided by Liu and colleagues[59] provide support for this concept. The authors performed extensive analysis of single cells in a mixed osteoblastic cell population and found extensive variation of the molecular phenotype among individual "osteoblastic cells" that can be explained by the variation in their functional abilities.[59]

The prospective use of the molecular signature to define the phenotype of clonal populations of hBMSC demonstrated the ability of these molecular markers to predict bone formation. However, we found that few clones were able to fulfill the criteria of expressing high levels of the five bone-related genes and low levels of immune-response genes or the opposite phenotype suggesting that most hBMSC clones may represent an inter-mediary phenotype and that, depending on culture conditions, they can be committed to different lineages. Examining the expression of the molecular signature in a large number of hBMSC clones is needed to confirm this hypothesis. Alternatively, additional gene markers need to be identified to improve the predictive value of this proposed molecular signature.

Our data demonstrate the presence of osteoblastic differentiation heterogeneity among cultured BMSCs populations and suggest that the currently employed hBMSCs surface markers, canonical osteoblastic markers, and the ex vivo mineralization assay lack the predictive power for identifying BMSC populations capable of in vivo bone forming (i.e., osteogenic BMSCs). Our findings suggest that osteogenic BMSCs cannot be identified by a limited number of canonical osteoblastic markers, but they should be identified by their ability to express a larger number of molecular markers important for in vivo bone formation. The molecular signature described here represents some of these possible markers, but several others remain to be identified. The availability of molecular markers may help in dissecting the functional heterogeneity of BMSCs and for prospective identification of osteogenic BMSC populations and their quality control prior to their use in clinical trials involving cell therapy for bone regeneration.

Disclosures

All the authors state that they have no conflicts of interest.

Acknowledgments

References

1. Bianco P, Robey PG, Simmons PJ. Mesenchymal stem cells: revisiting history, concepts, and assays. Cell Stem Cell. 2008;2:313–319.

2. Friedenstein AJ, Chailakhjan RK, Lalykina KS. The development of fibroblast colonies in monolayer cultures of guinea-pig bone marrow and spleen cells. Cell Tissue Kinet. 1970;3:393–403.

3. Kassem M, Mosekilde L, Eriksen EF. 1,25-Dihydroxyvitamin D_3 potentiates fluoride-stimulated collagen type I production in cultures of human bone marrow stromal osteoblast-like cells. J Bone Miner Res. 1993;8:1453–1458.

4. Kuznetsov SA, Krebsbach PH, Satomura K, et al. Single-colony derived strains of human marrow stromal fibroblasts form bone after transplantation in vivo. J Bone Miner Res. 1997;12:1335–1347.

5. Pittenger MF, Mackay AM, Beck SC, et al. Multilineage potential of adult human mesenchymal stem cells. Science. 1999;284:143–147.

6. Abdallah BM, Kassem M. Human mesenchymal stem cells: from basic biology to clinical applications. Gene Ther. 2008;15:109–116.

7. Quarto R, Mastrogiacomo M, Cancedda R, et al. Repair of large bone defects with the use of autologous bone marrow stromal cells. N Engl J Med. 2001;344:385–386.

8. Robey PG, Bianco P. The use of adult stem cells in rebuilding the human face. J Am Dent Assoc. 2006;137:961–972.

9. Parfitt AM. Bone forming cells in clinical conditions. In: Hall BK, ed. In Bone, The Osteoblast and Osteocyte. London: Telford Press; 1991: 351–426.

10. Calvi LM, Adams GB, Weibrecht KW, et al. Osteoblastic cells regulate the haematopoietic stem cell niche. Nature. 2003;425:841–846.

11. Aubin JE, Triffitt JT. Mesenchymal stem cells and osteoblast differentiation. In: Bilezikian JP, Raisz LG, Rodan GA, eds. The Principles of Bone Biology, 2nd edition. San Diego, CA: Academic Press; 2002: 59–81.

12. Rodan GA, Noda M. Gene expression in osteoblastic cells. Crit Rev Eukaryot Gene Expr. 1991;1:85–98.

13. Abdallah BM, Ditzel N, Kassem M. Assessment of bone formation capacity using in vivo transplantation assays: procedure and tissue analysis. Methods Mol Biol. 2008;455:89–100.

14. Dennis JE, Konstantakos EK, Arm D, Caplan AI. In vivo osteogenesis assay: a rapid method for quantitative analysis. Biomaterials. 1998;19:1323–1328.

15. Mankani MH, Kuznetsov SA, Fowler B, Kingman A, Robey PG. In vivo bone formation by human bone marrow stromal cells: effect of carrier particle size and shape. Biotechnol Bioeng. 2001;72:96–107.

16. Stenderup K, Rosada C, Justesen J, Al-Soubky T, Gnaes-Hansen F, Kassem M. Aged human bone marrow stromal cells maintaining bone forming capacity in vivo evaluated using an improved method of visualization. Biogerontology. 2004;5:107–118.

17. Djouad F, Bony C, Haupl T, et al. Transcriptional profiles discriminate bone marrow-derived and synovium-derived mesenchymal stem cells. Arthritis Res Ther. 2005;7:R1304–R1315.

18. Qi H, Aguiar DJ, Williams SM, La PA, Pan W, Verfaillie CM. Identification of genes responsible for osteoblast differentiation from human mesodermal progenitor cells. Proc Natl Acad Sci USA. 2003;100:3305–3310.

19. Scheideler M, Elabd C, Zaragosi LE, et al. Comparative transcriptomics of human multipotent stem cells during adipogenesis and osteoblastogenesis. BMC Genomics. 2008;9:340.

20. Schilling T, Noth U, Klein-Hitpass L, Jakob F, Schutze N. Plasticity in adipogenesis and osteogenesis of human mesenchymal stem cells. Mol Cell Endocrinol. 2007;271:1–117.

21. Song L, Webb NE, Song Y, Tuan RS. Identification and functional analysis of candidate genes regulating mesenchymal stem cell self-renewal and multipotency. Stem Cells. 2006;24:1707–1718.

22. Abdallah BM, Haack-Sorensen M, Burns JS, et al. Maintenance of differentiation potential of human bone marrow mesenchymal stem cells immortalized by human telomerase reverse transcriptase gene despite [corrected] extensive proliferation. Biochem Biophys Res Commun. 2005;326:527–538.

23. Simonsen JL, Rosada C, Serakinci N, et al. Telomerase expression extends the proliferative life-span and maintains the osteogenic potential of human bone marrow stromal cells. Nat Biotechnol. 2002;20:592–596.

24. Qiu W, Andersen TE, Bollerslev J, Mandrup S, Abdallah BM, Kassem M. Patients with high bone mass phenotype exhibit enhanced osteoblast differentiation and inhibition of adipogenesis of human mesenchymal stem cells. J Bone Miner Res. 2007;22:1720–1731.

25. Frederiksen CM, Knudsen S, Laurberg S, Orntoft TF. Classification of Dukes' B and C colorectal cancers using expression arrays. J Cancer Res Clin Oncol. 2003;129:263–271.

26. Irizarry RA, Bolstad BM, Collin F, Cope LM, Hobbs B, Speed TP. Summaries of Affymetrix GeneChip probe level data. Nucleic Acids Res. 2003; 31.

27. Al-Shahrour F, Minguez P, Vaquerizas JM, Conde L, Dopazo J. BABELOMICS: a suite of Web tools for functional annotation and analysis of groups of genes in high-throughput experiments. Nucleic Acids Res. 2005;33.

28. Gollner H, Dani C, Phillips B, Philipsen S, Suske G. Impaired ossification in mice lacking the transcription factor Sp3. Mech Dev. 2001;106: 77–83.

29. Chan YM, Bonnemann CG, Lidov HG, Kunkel LM. Molecular organization of sarcoglycan complex in mouse myotubes in culture. J Cell Biol. 1998;143:2033–2044.

30. Liu LA, Engvall E. Sarcoglycan isoforms in skeletal muscle. J Biol Chem. 1999;274:38171–38176.

31. Heyninck K, Beyaert R. Crosstalk between NF-κB-activating and apoptosis-inducing proteins of the TNF-receptor complex. Mol Cell Biol Res Commun. 2001; 4.

32. Hildebrand A, Romaris M, Rasmussen LM, et al. Interaction of the small interstitial proteoglycans biglycan, decorin and fibromodulin with transforming growth factor β. Biochem J. 1994;302:527–534.

33. Corsi A, Xu T, Chen XD, et al. Phenotypic effects of biglycan deficiency are linked to collagen fibril abnormalities, are synergized by decorin deficiency, and mimic Ehlers-Danlos-like changes in bone and other connective tissues. J Bone Miner Res. 2002;17:1180–1189.

34. Reinboth B, Hanssen E, Cleary EG, Gibson MA. Molecular interactions of biglycan and decorin with elastic fiber components: biglycan forms a ternary complex with tropoelastin and microfibril-associated glycoprotein 1. J Biol Chem. 2002;277:3950–3957.

35. Trask BC, Trask TM, Broekelmann T, Mecham RP. The microfibrillar proteins MAGP-1 and fibrillin-1 form a ternary complex with the chondroitin sulfate proteoglycan decorin. Mol Biol Cell. 2000;11: 1499–1507.

36. Raouf A, Ganss B, McMahon C, Vary C, Roughley PJ, Seth A. Lumican is a major proteoglycan component of the bone matrix. Matrix Biol. 2002; 21.

37. Raouf A, Seth A. Discovery of osteoblast-associated genes using cDNA microarrays. Bone. 2002;30:463–471.

38. Kim MS, Kim SS, Jung ST, et al. Expression and purification of enzymatically active forms of the human lysyl oxidase-like protein 4. J Biol Chem. 2003;278:52071–52074.

39. Maki JM, Sormunen R, Lippo S, Kaarteenaho-Wiik R, Soininen R, Myllyharju J. Lysyl oxidase is essential for normal development

and function of the respiratory system and for the integrity of elastic and collagen fibers in various tissues. Am J Pathol. 2005;167:927–936.

40. Wakitani S, Saito T, Caplan AI. Myogenic cells derived from rat bone marrow mesenchymal stem cells exposed to 5-azacytidine. Muscle Nerve. 1995;18:1417–1426.

41. Wewer UM, Ibaraki K, Schjorring P, Durkin ME, Young MF, Albrechtsen R. A potential role for tetranectin in mineralization during osteogenesis. J Cell Biol. 1994;127:1767–1775.

42. Potter LR, Bbey-Hosch S, Dickey DM. Natriuretic peptides, their receptors, and cyclic guanosine monophosphate-dependent signaling functions. Endocr Rev. 2006;27:47–72.

43. Matsukawa N, Grzesik WJ, Takahashi N, et al. The natriuretic peptide clearance receptor locally modulates the physiological effects of the natriuretic peptide system. Proc Natl Acad Sci USA. 1999;96:7403–7408.

44. Jaubert J, Jaubert F, Martin N, et al. Three new allelic mouse mutations that cause skeletal overgrowth involve the natriuretic peptide receptor C gene (Npr3). Proc Natl Acad Sci USA. 1999;96:10278–10283.

45. Hagiwara H, Inoue A, Yamaguchi A, et al. cGMP produced in response to ANP and CNP regulates proliferation and differentiation of osteoblastic cells. Am J Physiol. 1996;270:C1311–C1318.

46. Simonet WS, Lacey DL, Dunstan CR, et al. Osteoprotegerin: a novel secreted protein involved in the regulation of bone density. Cell. 1997;89:309–319.

47. Simeone A, Acampora D, Pannese M, et al. Cloning and characterization of two members of the vertebrate Dlx gene family. Proc Natl Acad Sci USA. 1994;91:2250–2254.

48. Lee MH, Kim YJ, Yoon WJ, et al. Dlx5 specifically regulates Runx2 type II expression by binding to homeodomain-response elements in the Runx2 distal promoter. J Biol Chem. 2005;280:35579–35587.

49. Puppin C, Fabbro D, Dima M, et al. High periostin expression correlates with aggressiveness in papillary thyroid carcinomas. J Endocrinol. 2008;197:401–408.

50. Gillan L, Matei D, Fishman DA, Gerbin CS, Karlan BY, Chang DD. Periostin secreted by epithelial ovarian carcinoma is a ligand for α(V)β(3) and α(V)β(5) integrins and promotes cell motility. Cancer Res. 2002;62:5358–5364.

51. Takeshita S, Kikuno R, Tezuka K, Amann E. Osteoblast-specific factor 2: cloning of a putative bone adhesion protein with homology with the insect protein fasciclin I. Biochem J. 1993;294:271–278.

52. Rios H, Koushik SV, Wang H, et al. Periostin null mice exhibit dwarfism, incisor enamel defects, and an early-onset periodontal disease-like phenotype. Mol Cell Biol. 2005;25:11131–11144.

53. Coutu DL, Wu JH, Monette A, Rivard GE, Blostein MD, Galipeau J. Periostin: a member of a novel family of vitamin K–dependent proteins is expressed by mesenchymal stromal cells. J Biol Chem. 2008;283:17991–18001.

54. Theill LE, Boyle WJ, Penninger JM. RANK-L and RANK: T cells, bone loss, and mammalian evolution. Annu Rev Immunol. 2002;20:795–823.

55. Mann GN, Jacobs TW, Buchinsky FJ, et al. Interferon-γ causes loss of bone volume in vivo and fails to ameliorate cyclosporin A–induced osteopenia. Endocrinology. 1994;135:1077–1083.

56. Nanes M, Rubin J, Titus L, Hendy G, Catherwood B. Interferon-γ inhibits 1,25-dihydroxyvitamin D_3–stimulated synthesis of bone GLA protein in rat osteosarcoma cells by a pretranslational mechanism. Endocrinology. 1990;127:588–594.

57. Takayanagi H, Sato K, Takaoka A, Taniguchi T. Interplay between interferon and other cytokine systems in bone metabolism. Immunol Rev. 2005;208:181–193.

58. Sacchetti B, Funari A, Michienzi S, et al. Self-renewing osteoprogenitors in bone marrow sinusoids can organize a hematopoietic microenvironment. Cell. 2007;131:324–336.

59. Liu F, Malaval L, Aubin JE. Global amplification polymerase chain reaction reveals novel transitional stages during osteoprogenitor differentiation. J Cell Sci. 2003;116:1787–1796.